Journal of
Ceramic Science
and Technology

J. Ceram. Sci. Technol. 19-26 (2019)
DOI: 10.4416/JCST2018-00071
available online at: http://www.ceramic-science.com

Integration of Piezoceramic Composites into Structural Components: Effect on the Polarisation State and Polarisability

K. Hohlfeld[1], S. Eßlinger[2], A. Eydam[3], A. Winkler[4], T. Weber[4], M. Gude[4], N. Modler[4], G. Gerlach[3], G. Suchaneck[3], A. Michaelis[1, 2], A. Schönecker[2], S. Gebhardt[2], P. Neumeister[*2]

[1]Technische Universität Dresden (TUD), Institute of Materials Science (IfWW), D-01062 Dresden, Germany
[2]Fraunhofer Institute for Ceramic Technologies and Systems (IKTS), Winterbergstraße 28, D-01277 Dresden, Germany
[3]Technische Universität Dresden (TUD), Solid State Electronics Laboratory (IFE), D-01062 Dresden, Germany
[4]Technische Universität Dresden (TUD), Institute of Lightweight Engineering and Polymer Technology (ILK), D-01062 Dresden, Germany

received June 26, 2018; received in revised form February 3, 2019; accepted February 18, 2019

Abstract

In lightweight construction, structural components with integrated piezoelectric sensors and actuators find application for condition monitoring, structural health monitoring, vibrational control, and reduction of noise emission. In order to create such multifunctional, so-called smart components, an integration technique for serial production, designed for embedding of piezofibre composites into thermoplastic structures, was developed recently. During the two-stage fabrication process, thermal and mechanical loads act on the piezoceramic, which can lead to partial depolarisation and thus degradation of the piezoelectric properties. Since the mechanical boundary conditions are significantly differing between the manufacturing stages, a direct determination and subsequent comparison of the piezoelectric values appears very difficult. Therefore, the effect of each process step of integration (here called integration step) on the polarisation state and polarisability of the piezofibre composites was investigated directly. The results indicate distinctive effects depending on the particular integration step. For the investigated integration technique, the overall depolarisation remains in a range which seems acceptable for low power applications such as sensing. However, for actuation the results suggest re-poling or poling after integration to assure maximum piezoelectric performance.

Keywords: Piezofibre composite, Integration, Polarisation state, Polarisability

I. Introduction

Smart components are gaining high interest in the fields of lightweight construction, automotive, and aerospace design. Piezoelectric sensors and actuators are combined with passive structures to utilize multifunctional applications like condition monitoring, structural health monitoring, vibrational control, or noise emission reduction in structures. Recently, a two-stage fabrication procedure for the direct integration of functional components into thermoplastic sheet structures has been developed, which allows for series production of active lightweight structures at low costs [1]. Therein, in the first process step of integration (here called integration step), functional components are positioned between two transparent thermoplastic carrier films and consolidated by hot-pressing, forming the thermoplastic-compatible piezoceramic module (TPM). In the second integration step, these TPMs are then integrated into a fibre-reinforced plastic (FRP) structure [2]. For the present investigations, 1 – 3 piezofibre composites (PFCs) consisting of a monolayer of PZT fibres embedded in epoxy resin were used as the functional components for the direct integration into thermoplastic sheet structures [3]. It is widely known from literature, that electromechanical properties of piezoelectric sensors and actuators are significantly affected by temperature as well as applied electrical and mechanical loads [4–12]. Since both thermal and mechanical loads occur during the two stages of the deployed fabrication procedure [1, 13, 14], the aim of the investigations was to evaluate the specific influence onto the properties of the integrated PFCs. From the material point of view, the piezoelectric properties of a ferroelectric material are primarily defined by its remanent polarisation state. We therefore investigated the effect of the fabrication processes on the polarisation state of the integrated piezoceramic composites. Furthermore, poling the material after a specific integration step might also be an option to reach maximum piezoelectric performance. Thus, we included a study on the polarisability of the embedded ferroelectric material. In order to account for different poling strategies during integration, two different sample types

* Corresponding author: peter.neumeister@ikts.fraunhofer.de

were manufactured. Including a reference series, we consider three sample groups:

I. reference samples, which were poled but not integrated,
II. pre-poled samples, which were poled only once before integration,
III. re-poled samples, which were additionally poled after each integration step.

Integration and investigation of the different sample groups was performed according to the experimental procedure depicted in Fig. 1. Thereby, the natural aging without the influence of fabrication processes and re-poling was deduced from the capacitance of the reference samples by means of impedance measurement (IM). The polarisation state was evaluated by the Laser Intensity Modulation Method (LIMM) [15, 16] and verified by comparison with results derived from the thermal pulse method. Therefore, the pyroelectric current was analysed by heating with an intensity-modulated laser beam or laser pulses [17]. Bipolar large-signal polarisation hysteresis measurements (HM) were performed to determine the effect of the integration on the polarisability.

After having given a short introduction and motivation of the present paper, the following methods section describes in detail the fabrication of the PFCs and their integration into thermoplastic sheet structures as well as the performed IM, LIMM and HM measurements. The observed results are reported and discussed in section three and the main findings summarised in the conclusions section.

II. Methods

(1) Sample Fabrication and Integration

(a) *Piezofibre composites (PFCs)*

Piezoceramic fibres were fabricated from PZT powder (SONOX® P505, CeramTec GmbH, Germany) by means of a phase inversion technology [18]. The sintered fibres with approximately 300 µm in diameter were then arranged in parallel as a monolayer and embedded into an epoxy resin (Araldite® 2020, Huntsman Advanced Materials, Switzerland). After curing, the resulting piezofibre composite (PFC) with lateral dimensions of 35 mm × 22 mm was ground to 250 µm thickness, leading to exposed fibre surfaces. Subsequently, continuous gold electrodes were deposited on top and bottom sides of the PFC by sputter coating. According to the fibre direction and the electrode design, the PFC utilizes a lateral d_{31} functionality. An example of such fabricated PFCs is shown in Fig. 2a.

(b) *First integration step: Integration of PFCs into thermoplastic-compatible piezoceramic modules (TPMs)*

For the first integration step, the PFCs were arranged between two thermoplastic foils (see Fig. 2b) forming thermoplastic-compatible piezoceramic modules (TPMs) [19]. The employed polyamide foils (PA6, 100 µm thickness) are metallised with a screen-printed net-like silver electrode pattern, which allows for reliable contact to the sputtered electrodes of the PFC. After inserting the PFC in between the two foils, the assembly was fixed by a local thermal welding process. Then, two self-adhesive copper strips were attached as contact elements on the upper and lower layer. Finally, the prepared structure was positioned between the sliders of an interval hot-pressing system and consolidated at 270 °C with a pressure of 3 bar over 15 s.

(c) *Second integration step: Integration of TPMs into fibre-reinforced polymers (FRP) with thermoplastic matrices*

The fibre-reinforced polymer (FRP) samples were manufactured using an adapted thermoforming technology (see Fig. 3). Pre-consolidated textile reinforced composite sheets, referred to as organic sheets, with a matrix made of polyamide 6 (PA6) and a glass fibre-reinforcement (TEPEX® 102-RG600(x)/47%, Bond Laminates GmbH) and a thickness of 2 mm were used. The organic sheets were fixed in a stentering frame and heated up to 290 °C in an infrared preheating station. Then they were transferred into a pressing die within 6 s. Thus, the organic sheet has a temperature of approx. 270 °C at the beginning of the pressing process, which is significantly higher than the melting temperature of the PA 6 matrix (T_M = 223 °C). A thermoplastic film assembled with a TPM was fixed in the upper die adopting the 110 °C temperature of the constantly

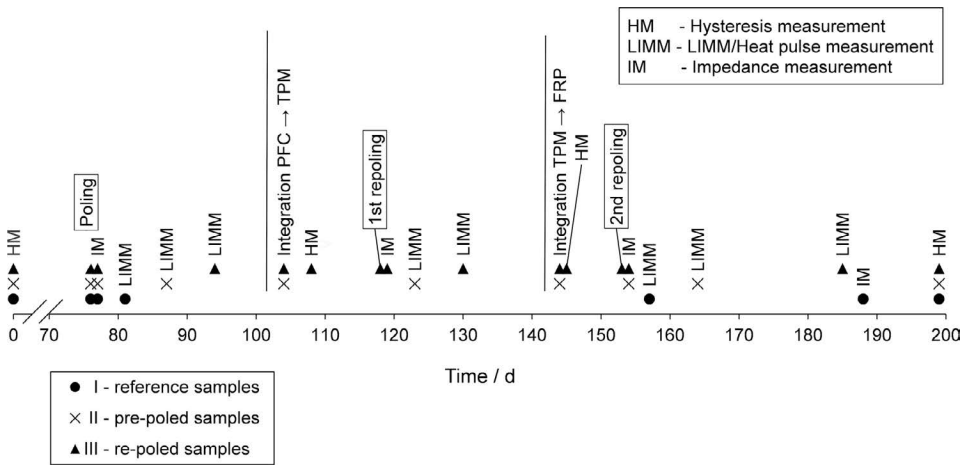

Fig. 1: Fabrication and measurements procedure timetable.

tempered pressing die. The surface of the pressing die was coated with a silicone layer (thickness 2 mm) in order to assure homogeneous pressing stresses in the piezoceramic during the pressing process. After the insertion of the organic sheet into the press, the tool was closed immediately and a pressure of 0.01 MPa was applied to the components. Thus, the thermoplastic components of the organic sheet, the thermoplastic foil, and the carrier films of the TPM melted together. The appropriate dwell time for this consolidation was 130 s. After cooling to tool temperature within 80 s and under constant pressure, the press was opened and the FRP with integrated TPM was removed (see Fig. 2c).

(d) ***Poling***

Initial poling was performed by exposing each PFC to an electrical field of 2 kV/mm for 5 minutes at 80 °C temperature. For group III samples, re-poling was performed with identical parameters after each integration step (see Fig. 1).

(2) Measurements

(a) ***Electrical Capacity***

In practice, the permittivity of a piezoelectric ceramic or its change during poling is typically used as measure for the polarisation state. A simple evaluation of the permittivity of the ceramic fibres is difficult due to the composite structure. Therefore, the electrical capacity C of the samples was determined with an impedance analyzer (HP 4194A with test fixture 16034E). A sinusoidal voltage signal with a frequency of 1 kHz and a voltage amplitude of 0.5 V was applied at room temperature.

(b) Polarisation State

The polarisation state of the samples was evaluated non-destructively by Laser Intensity Modulation Method (LIMM) [15]. The pyroelectric response of a harmonically heated piezoelectric plate exhibiting heat losses to the environment is characterized by the thermal relaxation time τ_{th} of the piezoelectric plate, the average pyroelectric coefficient p_0 and the spatially dependent parts p_n of the pyroelectric coefficient [16, 20, 21]. The coefficients p_n are generally small for commercially available homogeneously poled piezoelectric plates [22]. Suitable information for the application of piezoelectric transducers is limited to the frequency range below 100 Hz [23–25].The actual amount of absorbed laser radiation can only be estimated, so an absolute value of the pyroelectric coefficient cannot be calculated. The laser radiation is absorbed by the gold electrode of the PFC. This fact also applies to the integrated samples because the top PA 6 film is almost translucent.

Furthermore, it is assumed that the effect of the film on the periodic temperature fields within the piezo-composite can be neglected. Consequently, the same amount of laser radiation is absorbed by the samples in the three states PFC, TPM and FRP, enabling a direct comparison of the pyroelectric current.

The thermal relaxation time of PZT fibres embedded in epoxy resin exceeds a few seconds. Thus, the thermal losses occur in a frequency range below 0.1 Hz. Thus, the pyroelectric current I yields in the frequency region from 0.1 Hz to 100 Hz:

$$I(\omega) \approx \frac{\Phi_0 A}{c\rho \cdot d} p_0 \tag{1}$$

where Φ_0 is the heat flux absorbed by the plate surface, A the heated area, c the specific heat, ρ the density and d the thickness of the piezoelectric plate.

At higher frequencies, the piezoelectric material causes also electromechanical resonances [26].

The results of [27] indicate that p and P_r can be assumed proportional and are related by:

$$p = \frac{P_r \cdot \varepsilon_r}{C_C} \tag{2}$$

following an empirical extended Curie-Weiß law, where ε_r is the relative permittivity and C_C the Curie constant. Inserting eq. (2) into eq. (1), a relation for the comparison of the remanent polarisation P_r of a sample at different times i and k, i.e. integration states, can be deduced:

$$\frac{P_{r,k}}{P_{r,i}} \approx \frac{I_k \cdot \varepsilon_{r,i}}{I_i \cdot \varepsilon_{r,k}} \tag{3}$$

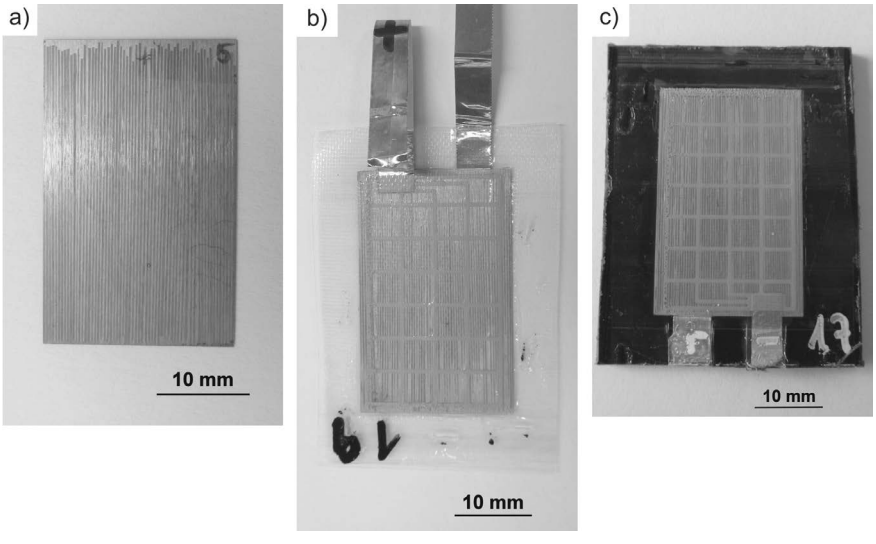

Fig. 2: Fabricated samples: a) initial PFC, b) after integration PFC → TPM, c) after integration TPM → FRP.

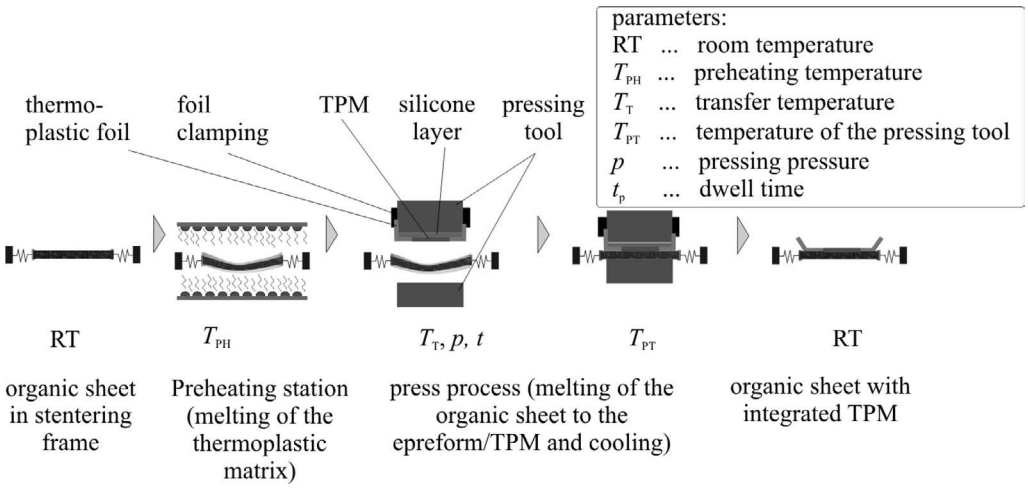

Fig. 3: Schematic thermoforming process for the integration of TPM in FRP with thermoplastic matrices.

LIMM measurements were performed by heating the samples periodically with a single laser diode (LCU98A041A, Laser Components GmbH, Olching, Germany) square-wave-modulated in the frequency range from 100 mHz up to 1 kHz with a power of 12 mW at a wavelength of 980 nm. The complex pyroelectric current was determined by an impedance/gain-phase analyzer (Solartron 1260, Solartron Analytical, Farnborough, UK) with DC coupling. In order to reduce noise, 30 measurement repetitions were used for averaging. Furthermore, the effective permittivities ε_r of the PFCs were derived from the electrical capacity measurements.

Additionally, thermal pulse measurements were carried out by heating the samples with a pulsed laser diode (LC905D3S3J09S, Laser Components GmbH, Olching, Germany) at a wavelength of 905 nm with a peak power of 55 W, a pulse width of 100 ns and a repetition frequency of 1 Hz. The pyroelectric current was transformed to a voltage by a current amplifier (SR570, Stanford Research Systems, Sunnyvale, CA) and filtered by an in-house-built 50 Hz notch filter before recording by a Waverunner® Xi-A oscilloscope (LeCroy, Chestnut Ridge, USA) with DC coupling.

The voltage signal in time domain was converted to the frequency domain by a discrete fast Fourier transform. The obtained frequency spectrum was divided by the transfer function of the measurement set-up to account for the influence of the amplifier settings. The thermal pulse approach is described in detail in [28].

(c) *Polarisability*

Polarisation hysteresis measurements were conducted on the different samples at room temperature. Ten bipolar electric cycles with an amplitude of 2 kV/mm were applied, from which the last was evaluated. A Sawyer-Tower circuit was used to capture the electric charges [29]. A net polarisation P is computed from the charges Q by means of the active area A of each PFC and accounting for the non-material contribution of the electric field to the charges:

$$P=\frac{Q}{A}-\frac{\varepsilon_0 \cdot U}{d} \quad (4)$$

Therein, ε_0, U and d represent the vacuum permittivity, the applied voltage and the electrode distance, respectively.

The PZT 5A material (Type 200 piezoceramic in accordance with European Standard EN 50324 – 1) used in this investigation shows a more complex behaviour: the hysteresis is shifted along the electric field axis against the direction of the initial poling field (Fig. 4). This leads to a non-symmetric hysteresis loop for symmetric bipolar loading. Therefore, when evaluating a pre-poled sample, it is not possible to determine the absolute polarisation. Hence, only the change in remanent polarisation can be evaluated.

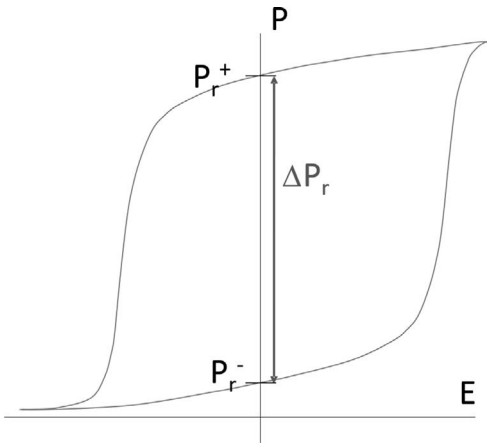

Fig. 4: Schematic polarisation hysteresis loop of a PZT 5A ceramic, showing a hysteresis shift (initial poling in negative electric field direction).

For the evaluation of the remanent polarisability of the piezoceramic the use of the change in remanent polarisation due to re-poling ΔP_r at zero electric field is proposed. It is calculated as follows:

$$\Delta P_r = P_r^+ - P_r^- \quad (5)$$

III. Results and Discussion

The electrical capacity C was determined by means of impedance measurements (IM) for the different sample groups before as well as after the integration steps (see Fig. 1). The results are depicted in Fig. 5. Reference samples, which were not integrated, show a slight decrease of capacity values over time (< 4% in 122 d). This is assumed as natural degradation of the used PFC or piezo material, respectively [30]. The capacity of pre-poled sam-

ples remains almost stable for the first integration step (PFC→TPM) and undergoes a slight decrease (< 4%) for the second (TPM→FRP). Re-poled samples exhibit a decrease of capacity values of < 4% for the first integration as well as approximately 6% in sum after the second integration.

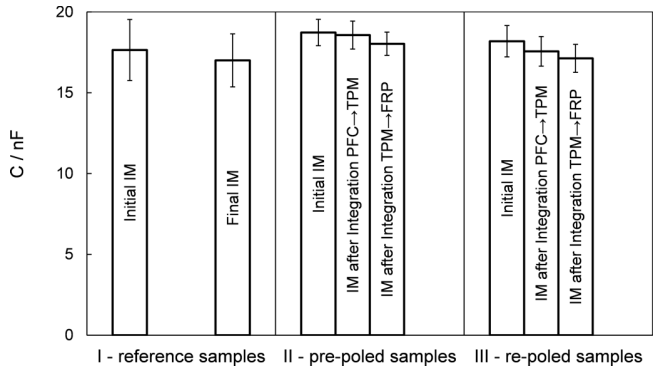

Fig. 5: Change in capacity (from impedance measurement IM) for samples I, II, III at different integration steps.

Figures 6 and 7 show the pyroelectric current spectra of a pre-poled and a re-poled sample, respectively, in the three states PFC, TPM and FRP as result of LIMM measurements. In the frequency range from 1 Hz to 100 Hz, the real part is almost constant and the imaginary part is negligible. The pyroelectric current of the pre-poled sample decreases after each integration step in contrast to the re-poled sample.

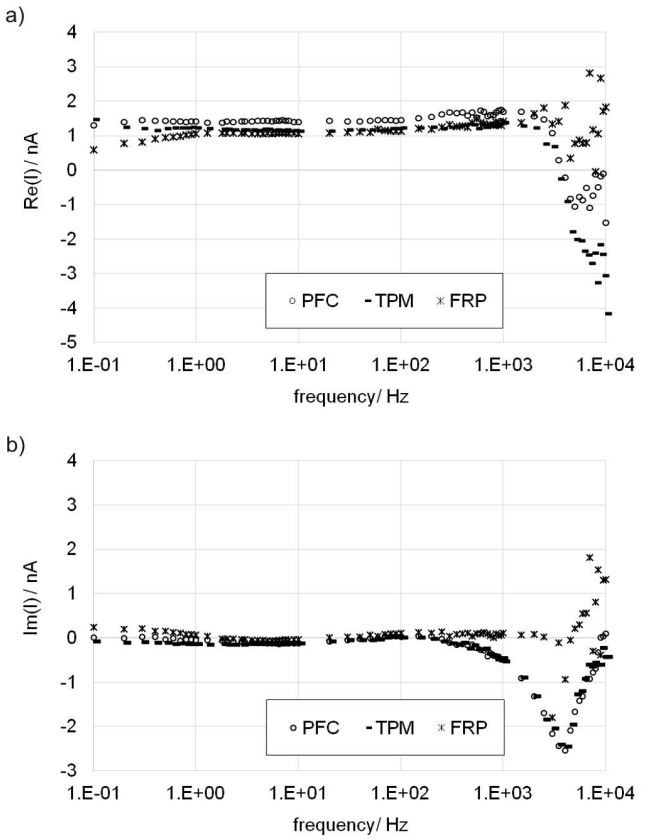

Fig. 6: (a) Real and (b) imaginary parts of the pyroelectric current spectra for a pre-poled sample (II) in the three states PFC, TPM and FRP.

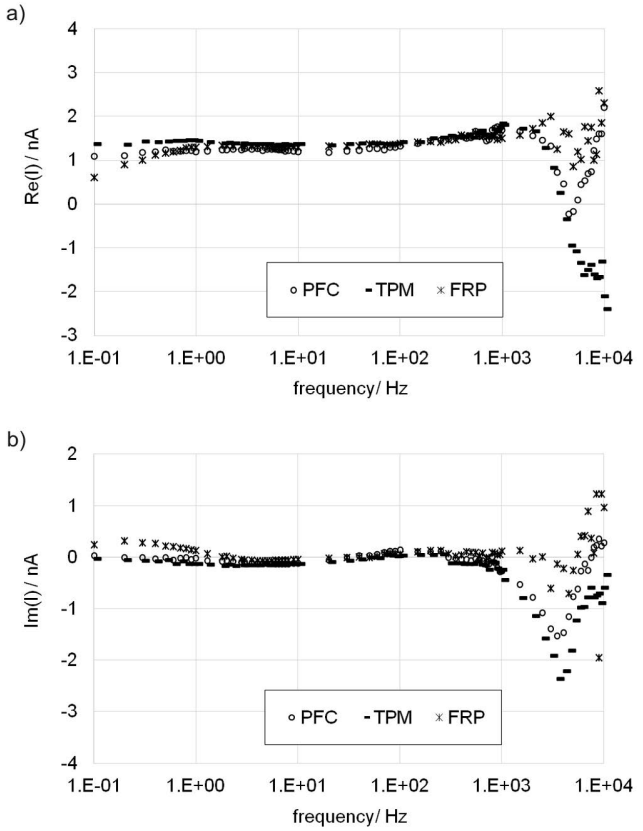

Fig. 7: (a) Real and (b) imaginary parts of the pyroelectric current spectra for a re-poled sample (III) in the three states PFC, TPM and FRP.

Table 1 presents the ratios of the remanent polarisation after a process step to that before for the pre-poled and the re-poled samples as well as the polarisation ratio over time for the reference samples according to Eq. (3) (see also Fig. 1). The values (of each group) were not averaged due to the observed sample variation. The remanent polarisation of the reference samples (I) remained stable over time. One sample exhibited an increase of 11%. All pre-poled samples (II) showed a degradation of the remanent polarisation after each integration step. The range of degradation varied widely between 1% and 23% for one integration step. The measurement uncertainty of $P_{r,k}/P_{r,i}$ amounted to ± 4% for a confidence interval of 95%. Furthermore, the polarisation of the re-poled samples (III) was increased after the first integration step and slightly decreased after the second one. Overall polarisation ratios of re-poled samples were observed to be higher (97% - 111%) than those of pre-poled samples (64% - 83%).

Using the thermal pulse method, the pyroelectric response had to be measured discretely in four different bandwidths from 1 Hz - 15 Hz up to 1 kHz - 20 kHz to cover a wide frequency range. Combination of the resulting spectra allowed for a comparison with the LIMM results. In general, the real parts of the obtained spectra were in good agreement with the LIMM spectra for all PFC samples (an example is shown in Fig. 8), but best for the 10 Hz - 200 Hz bandwidth. With regard to the effect of integration on the PFCs, investigations were performed with this bandwidth. Figure 9 presents the compared spectra for a pre-poled sample in the three states

Table 1: Ratios of the remanent polarisation after integration (group II, III) as well as over time (group I).

$P_{r,k}/P_{r,i}$ (%)					
Sample group	No.	Integration PFC→TPM	Integration TPM→FRP	Overall PFC→FRP	Final PFC/Initial PFC
I – reference samples	3				101
	4				100
	5				111
II – pre-poled samples	6	99	82	81	
	7	83	77	64	
	8	97	86	83	
	10	81	94	75	
III – re-poled samples	14	113	99	111	
	17	125	78	97	
	18	113	91	103	
	19	113	97	110	

PFC, TPM and FRP. The thermal pulse response shows the same trend as the results obtained by LIMM, however, the spectra are noisier. The heat pulse is distributed over the whole frequency spectrum, whereas with LIMM, 55 frequency points are measured separately between 0.1 Hz and 1 kHz, collecting a much larger amount of data. On the contrary, the measurement duration using thermal pulse method could be reduced approximately by a factor of 50 compared to LIMM.

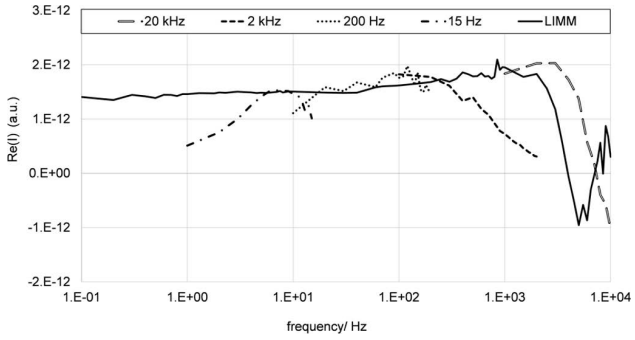

Fig. 8: Real parts of the pyroelectric current spectra of a PFC sample (I) for four different bandwidths in comparison to the LIMM spectrum.

Fig. 10 depicts the averaged change in remanent polarisation ΔP_r and its standard deviation for the observed sample groups. The reference samples (I) show an increase in polarisation to 108% from the initial hysteresis measurement compared to the final hysteresis measurement (see also Fig. 1). The pre-poled (II) samples show a decrease of polarisability to 95% as result of the two-stage integration process. For the re-poled (III) samples, the influence of the specific integration step can be seen, e.g. an increase of ΔP_r after the first integration step. This can be attributed to a beneficial influence of slight mechanical prestress during polarisation [10, 11] due to the integration state. As expected, the re-poled samples (III) show an overall decrease of polarisability to 95%, similar to the pre-poled samples (II), since both sample groups were integrated equally. In summary, the polarisability of the PFCs is only slightly affected by the employed fabrication procedure.

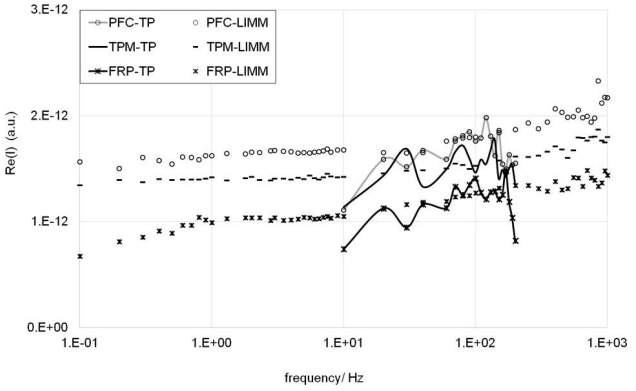

Fig. 9: Comparison of the real parts of the pyroelectric current spectra of a pre-poled sample (II) in the three states PFC, TPM and FRP obtained by the thermal pulse method (TP) for 10 Hz to 200 Hz and by LIMM.

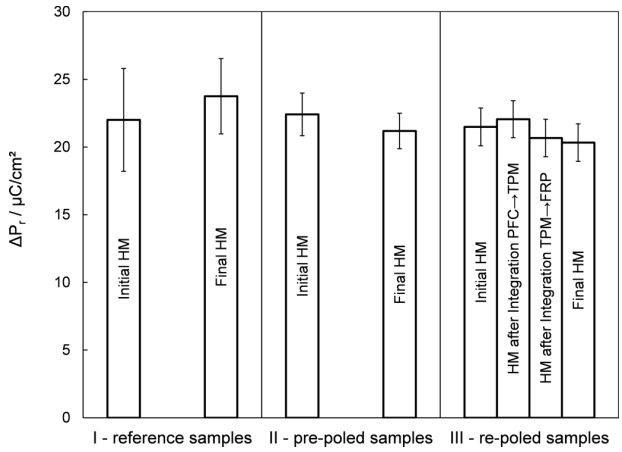

Fig. 10: Change in remanent polarisation ΔP_r (from hysteresis measurements HM) for sample group I, II, III.

IV. Conclusions

Piezofibre composites (PFCs) were integrated into thermoplastic structures using a two-stage process. First, they were arranged between two functionalised thermoplastic foils and hot-pressed to form a thermoplastic-compatible piezoceramic module (TPM). Then, the TPM was further integrated into a fibre-reinforced plastic (FRP) structure. The electrical capacity, polarisation state, and polarisability were investigated for each integration step to estimate the effect on the piezoelectric properties.

LIMM experiments showed a degradation of the remanent polarisation after integration. The range of degradation of pre-poled samples varied widely between 1% and 23% for each integration step. In contrast, the polarisation state of the re-poled samples was increased or only slightly decreased. The results indicate that the first integration step (PFC→TPM) has less impact on the remanent polarisation than the second one (TPM→FRP). LIMM experiments were confirmed by thermal pulse results. Impedance measurements exhibited a decrease of capacity of 4% - 6% for all sample groups. The observed changes in polarisation were not captured by the capacity measurements.

The attainable remanent polarisation charge decreased after integration. The remanent polarisability of the integrated composites reached 95% of the initial value.

During integration, the polarisation state of the pre-poled PFCs was preserved for the most part (64% - 83%). However, re-poling or poling subsequently to integration promises highest remanent polarisation and thus piezoelectric performance.

Acknowledgement

This research is supported by the Deutsche Forschungsgemeinschaft (DFG) in context of the Collaborative Research Centre/Transregio 39 PT-PIESA, subprojects A01, A05, B04, C03 and C08.

References

1 Hufenbach, W., Modler, N., Winkler, A., Ilg, J., Rupitsch, S. J.: Fibre-reinforced composite structures based on thermoplastic matrices with embedded piezoceramic modules, *Smart Mater. Struct.*, **23**, 025011, (2014).

2 Hufenbach, W., Gude, M., Modler, N., Heber, Th., Winkler, A., Weber, T.: Process chain modeling and analysis for the high-volume production of thermoplastic composites with embedded piezoceramic modules, *Smart Mater. Res.*, **2013**, 201631, (2013).

3 Hohlfeld, K., Neumeister, P., Michaelis, A., Gebhardt, S.: Tailored composite transducers based on piezoceramic fibers and pearls, In: Proceedings ACTUATOR 2016, June 13 – 15, Bremen, 69 – 72, 2016.

4 Damjanovic, D.: Stress and frequency dependence of the direct piezoelectric effect in ferroelectric ceramics, *J. Appl. Phys.*, **82**, 1788 – 1797, (1997).

5 Yang, G., Mukherjee, B. K.: The stress dependence of the piezoelectric d coefficient of piezoelectric and electrostrictive ceramic materials, *J. Acoust. Soc. Am.*, **106**, 2122, (1999).

6 Zhao, J., Glazounov, A. E., Zhang, Q. M.: Change in electromechanical properties of 0.9PMN:0.1PT relaxor ferroelectric induced by uniaxial compressive stress directed perpendicular to the electric field, *Appl. Phys. Lett.*, **74**, 436 – 438, (1999).

7 Fan, J., Stoll, W. A., Lynch, C. S.: Nonlinear constitutive behavior of soft and hard PZT: Experiments and modeling, *Acta Mater.*, **47**, 4415 – 4425, (1999).

8 Chaplya, P. M., Carman, G. P.: Dielectric and piezoelectric response of lead zirconate-lead titanate at high electric and mechanical loads in terms of non-180° domain wall motion, *J. Appl. Phys.*, **90**, 5278, (2001).

9 Mauck, L. D., Lynch, C. S.: Thermo-electro-mechanical behavior of ferroelectric materials, Part I: A computational micromechanical model versus experimental results, *J. Intel. Mater. Sys. Struct.*, **14**, pp. 587 – 602, (2003).

10 Zhou, D., Kamlah, M., Munz, D.: Effects of uniaxial prestress on the ferroelectric hysteretic response of soft PZT, *J. Eur. Ceram. Soc.*, 25 (4), 425 – 432, (2005).

11 Nicolai, M.: (Poling behaviour of piezoceramics under combined electrical, mechanical, and thermal stress) Polarisierungsverhalten von Piezokeramik unter kombinierter elektrischer, mechanischer und thermischer Beanspruchung, (Phd thesis) Dissertation Technische Universität Dresden, Dresden, 2012.

12 Neumeister, P., Eßlinger, S., Gebhardt, S., Schönecker, A., Flössel, M.: Effect of mechanical constraints in thin ceramic LTCC/PZT multilayers on the polarization behavior of the embedded PZT, *Int. J. Appl. Ceram. Technol.*, **11**, 422 – 430, (2014).

13 Winkler, A.: (Series-compatible design and manufacturing techniques of functional integrated thermoplastic fiber-reinforced plastic parts with embedded piezoceramic modules) Seriengerechte Bauweisen und Fertigungstechnologien für funktionsintegrative thermoplastische Faserverbundbauteile mit eingebetteten Piezokeramik-Modulen, Dissertation (Phd thesis), Technische Universität Dresden, Dresden, (2016).

14 Hohlfeld, K. et al.: Effect of the integration of piezoceramic composites into structural components on their poling condition and polarizability, In: VIII ECCOMAS Thematic Conference on Smart Structures and Materials SMART 2017, 5 – 8 June 2017, Madrid, Spain, Eds. A. Güemes, A. Benjeddou, J. Rodellar and J. Leng. Barcelona: International center for numerical methods in engineering (CIMNE): 349 – 358, 2017, ISBN: 978 – 84 – 946909 – 3-8.

15 Lang, S.B., Das-Gupta, D.K.: Laser-intensity-modulation method: a technique for determination of spatial distributions of polarization and space charge in polymer electrets, *J. Appl. Phys.*, **59**, 2151-2160, (1986).

16 Ploss, B., Emmerich, R., Bauer, S.: Thermal wave probing of pyroelectric distributions in the surface region of ferroelectric materials: a new method for the analysis, *J. Appl.Phys.*, **72**, 5363-5370, (1992).

17 Eydam, A., Suchaneck, G., Hohlfeld, K., Gebhardt, S., Michaelis, A., Gerlach, G.: Evaluation of the polarization state of piezofiber composites, In: Proceedings IEEE Joint ISAF-PFM 2013, 190 – 193, Prag, Czech Republic, 2013.

18 Hohlfeld, K., Gebhardt, S., Schönecker, A., Michaelis, A.: PZT components derived from polysulphone spinning process, *Adv. Appl. Ceram.*, **114**, 231 – 237, (2015).

19 Heber, Th., Gude, M., Hufenbach, W.: Production process adapted design of thermoplasticcompatible piezoceramic modules, Composites: Part A. **59**, 70 – 77, (2014).

20 Bauer, S., Ploss, B.: A method for the measurement of the thermal, dielectric, and pyroelectric properties of thin pyroelectric films and their applications for integrated heat sensors, *J. Appl. Phys.*, **68**, 6361 – 6367, (1990).

21 Carslaw, H. S., Jaeger, J. C.: Conduction of heat in solids, 2nd ed., New York, NY: Oxford University Press, (1959).

22 Eydam, A., Suchaneck, G., Eßlinger, S., Schönecker, A., Neumeister, P., Gerlach, G.: Polarization characterization of PZT disks and of embedded PZT plates by thermal wave methods, In: AIP Conf. Proceedings **1627**, 31 – 36, (2014).

[23] Suchaneck, G., Eydam, A., Hu, W., Krantz, B., Drossel, W.-G., Gerlach, G.: Evaluation of polarization of embedded piezoelectrics by the thermal wave method, IEEE Tran. Ultrason. Ferroelectr. Freq. Control, **59**, 1950 – 1954, (2012).

[24] Suchaneck, G., Eydam, A., Rübner, M., Schwankl, M., Gerlach, G.: A simple thermal wave method for the evaluation of the polarization state of embedded piezoceramics, *Ceram. Int.*, **39**, 587 – 590, (2013).

[25] Eydam, A., Suchaneck, G., Schwankl, M., Gerlach, G., Singer, R. F., Körner, C.: Evaluation of polarization state of light metal embedded piezoelectrics, Advances in Applied ceramics **114**, 226 – 230, (2015).

[26] Bauer, S., Bauer-Gogonea, S.: Current practice in space charge and polarization profile measurements using thermal techniques, IEEE Trans. Diel. Electr. Insul. **10**, 883 – 902, (2003).

[27] Liu, S. T., Zook, J. D.: Evaluation of curie constants of ferroelectric crystals from pyroelectric response, Ferroelectrics **7**, 171 – 173, (1974).

[28] Eydam, A., Suchaneck, G., Gerlach, G.: Non-destructive evaluation of integrated piezoelectric transducers by thermal waves and thermal pulses, In: 3rd International Conference on System-Integrated Intelligence: New Challenges for Product and Production Engineering 2016, Proceedia Technology, **26**, 59 – 65, 2016.

[29] Sawyer, C. B., Tower, C. H.: Rochelle salt as a dielectric, *Phys. Rev.*, **35**, 269 – 275, (1930).

[30] CeramTec Datasheet 'Materials for actuators', SONOX® P505, CeramTec GmbH, Lauf, Germany, (2017).